

# On the self-magnetostatic energy of jagged domain walls

Cite as: Journal of Applied Physics **66**, 3727 (1989); <https://doi.org/10.1063/1.344057>

Submitted: 09 December 1988 . Accepted: 13 June 1989 . Published Online: 27 October 1998

M. Mansuripur



View Online



Export Citation

## Ultra High Performance SDD Detectors



See all our XRF Solutions

# On the self-magnetostatic energy of jagged domain walls

M. Mansuripur

Optical Sciences Center, University of Arizona, Tucson, Arizona 85721

(Received 9 December 1988; accepted for publication 13 June 1989)

The demagnetizing energy of thin magnetic films can be written in terms of the Fourier components of the magnetization distribution. This formalism is used to investigate the structure of jagged domain walls in both perpendicular and in-plane media. Also introduced is a set of correlation functions and their relationship to demagnetizing energy density in media with random magnetization distribution.

## I. DEMAGNETIZING ENERGY OF JAGGED WALLS

The jaggedness of transition regions in magnetic recording is a major source of jitter noise in readout. In an attempt to better understand the magnetostatic origins of jaggedness, we have studied a simple model of the transition region. The analysis is based on an expression for the self- (demagnetizing) energy density of thin films in the Fourier domain which is written as<sup>1</sup>

$$E_M = 2\pi \sum_{n=-\infty}^{\infty} \sum_{m=-\infty}^{\infty} \{G(hf) |\mathbf{M}_{mn} \cdot \hat{z}|^2 + [1 - G(hf)] |\mathbf{M}_{mn} \cdot \hat{\sigma}_{mn}|^2\}. \quad (1a)$$

In Eq. (1a) the magnetostatic energy per unit volume is denoted by  $E_M$ . The magnetic film of thickness  $h$  has dimensions  $L_x \times L_y$  in the  $xy$  plane; its magnetization distribution  $\mathbf{M}(x,y)$  is uniform through the thickness but arbitrary otherwise. To simplify the analysis, periodic boundary conditions have been assumed, namely, the  $xy$  plane is completely covered with identical  $L_x \times L_y$  tiles. The Fourier components of magnetization distribution are therefore given by

$$\mathbf{M}_{mn} = \frac{i}{L_x L_y} \int_0^{L_x} \int_0^{L_y} \mathbf{M}(x,y) \times \exp\left[-i2\pi\left(\frac{mx}{L_x} + \frac{ny}{L_y}\right)\right] dx dy. \quad (1b)$$

The  $x$  and  $y$  components of frequency in the Fourier domain are  $f_x = m/L_x$  and  $f_y = n/L_y$ . The magnitude of the frequency vector  $\mathbf{f}$  is  $f = \sqrt{f_x^2 + f_y^2}$  and the unit vector  $\hat{\sigma}_{mn}$  is in the direction of  $\mathbf{f}$ , i.e.,

$$\hat{\sigma}_{mn} = (f_x/f)\hat{x} + (f_y/f)\hat{y}. \quad (1c)$$

Finally, the function  $G(\cdot)$  in Eq. (1a) is a low-pass spatial filter with circular symmetry that is given by

$$G(r) = \exp(-\pi r) [\sinh(\pi r)/\pi r]. \quad (1d)$$

Note that the width of the filter is inversely proportional to the film thickness  $h$ . A plot of the function  $G(hf)$  is shown in Fig. 1. According to Eq. (1a), therefore, the perpendicular components of magnetization contribute to demagnetizing energy after going through a low-pass filter, while the in-plane components contribute after going through a high-pass filter.

Let us now consider an array of walls, all parallel to the  $y$  axis, with an arbitrary amount of jaggedness in each wall as shown in Fig. 2. For simplicity we assume a sinusoidal magnetization distribution where  $\mathbf{M}(x,y)$  has the following

three components in the Cartesian coordinate system:

$$\mu_1(x,y) = |\mathbf{M}| \cos\left[\frac{2\pi}{L_x}\left(x + \alpha \sin\frac{2\pi y}{L_y}\right)\right], \quad (2a)$$

$$\mu_2(x,y) = |\mathbf{M}| \sin\left[\frac{2\pi}{L_x}\left(x + \alpha \sin\frac{2\pi y}{L_y}\right)\right] \cos\phi_0, \quad (2b)$$

$$\mu_3(x,y) = |\mathbf{M}| \sin\left[\frac{2\pi}{L_x}\left(x + \alpha \sin\frac{2\pi y}{L_y}\right)\right] \sin\phi_0. \quad (2c)$$

In these equations  $|\mathbf{M}|$ , a constant, is the magnitude of the magnetization vector,  $\alpha$  and  $L_y$  are the amplitude and the period of jaggedness, respectively,  $L_x$  is the period of the wall pairs, and  $\phi_0$  is a constant angle which determines the relative magnitudes of  $\mu_2$  and  $\mu_3$ . By assigning the three components of  $\mathbf{M}$  to the  $x$ ,  $y$ , and  $z$  axes in various orders, one obtains several types of  $180^\circ$  walls as follows:

(i) in-plane head-to-head wall:

$$\mathbf{M} = \mu_1\hat{x} + \mu_2\hat{y} + \mu_3\hat{z}, \quad (3a)$$

(ii) in-plane side-by-side wall:

$$\mathbf{M} = \mu_3\hat{x} + \mu_1\hat{y} + \mu_2\hat{z}, \quad (3b)$$

(iii) perpendicular wall:

$$\mathbf{M} = \mu_2\hat{x} + \mu_3\hat{y} + \mu_1\hat{z}. \quad (3c)$$

The three components of  $\mathbf{M}(x,y)$  in Eq. (2) have the

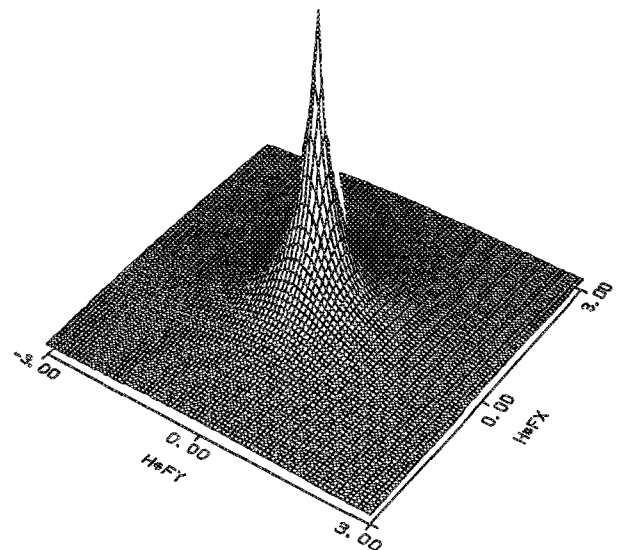


FIG. 1. A plot of the function  $G(hf)$  in the  $f_x, f_y$  frequency plane.

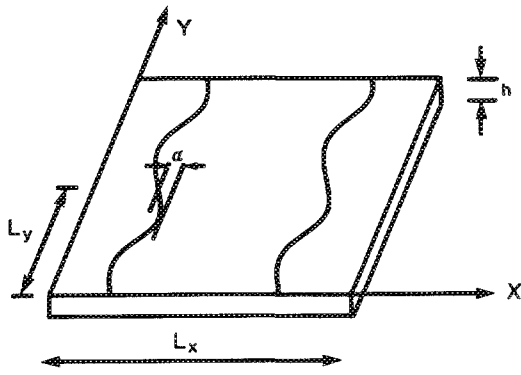


FIG. 2. A pair of jagged walls in a magnetic film of thickness  $h$ .  $L_y$  and  $\alpha$  are the period and the amplitude of jaggedness, respectively.

following Fourier coefficients:

$$\mathbf{M}_{mn}^{(1)} = \frac{1}{2} |\mathbf{M}| J_n(2\pi m \alpha / L_x);$$

$$m = \pm 1, \quad n = 0, \pm 1, \pm 2, \dots, \quad (4a)$$

$$\mathbf{M}_{mn}^{(2)} = (m/2i) |\mathbf{M}| J_n(2\pi m \alpha / L_x) \cos \phi_0;$$

$$m = \pm 1, \quad n = 0, \pm 1, \pm 2, \dots, \quad (4b)$$

$$E_M = \pi |\mathbf{M}|^2 \left[ \sum_{n=-\infty}^{\infty} G(h \sqrt{(1/L_x)^2 + (n/L_y)^2}) J_n^2\left(\frac{2\pi \alpha}{L_x}\right) \sin^2 \phi_0 \right. \\ \left. + \sum_{n=-\infty}^{\infty} \{1 - G[h \sqrt{(1/L_x)^2 + (n/L_y)^2}]\} J_n^2\left(\frac{2\pi \alpha}{L_x}\right) \left( \frac{(1/L_x)^2 + (n/L_y)^2 \cos^2 \phi_0}{(1/L_x)^2 + (n/L_y)^2} \right) \right]. \quad (7)$$

In the absence of jaggedness  $\alpha = 0$  and the energy density can be written simply as

$$E_M = \pi |\mathbf{M}|^2 \{G(h/L_x) \sin^2 \phi_0 + [1 - G(h/L_x)]\}. \quad (8)$$

The best choice for  $\phi_0$  in this case is  $\phi_0 = 0$  so that the magnetization remains entirely in the plane of the film. Now, as  $\alpha$  increases  $\phi_0$  tends towards  $90^\circ$ . The reason is that in the expression for the energy of the perpendicular component [first summation in Eq. (7)] the term with  $n = 0$  decreases with increasing  $\alpha$  (the first zero of  $J_0$  is at  $\alpha \approx 0.38L_x$ ). The other terms with  $n \neq 0$  are also small (assuming  $L_y \ll L_x$ ) because the filter function  $G(hf)$  is small at high frequen-

$$E_M = \pi |\mathbf{M}|^2 \left[ \sum_{n=-\infty}^{\infty} G[h \sqrt{(1/L_x)^2 + (n/L_y)^2}] J_n^2\left(\frac{2\pi \alpha}{L_x}\right) \cos^2 \phi_0 \right. \\ \left. + \sum_{n=-\infty}^{\infty} \{1 - G[h \sqrt{(1/L_x)^2 + (n/L_y)^2}]\} J_n^2\left(\frac{2\pi \alpha}{L_x}\right) \left( \frac{(1/L_x)^2 \sin^2 \phi_0 + (n/L_y)^2}{(1/L_x)^2 + (n/L_y)^2} \right) \right]. \quad (9)$$

In the absence of jaggedness  $\alpha = 0$  and the energy density is simply written

$$E_M = \pi |\mathbf{M}|^2 \{G(h/L_x) \cos^2 \phi_0 \\ + [1 - G(h/L_x)] \sin^2 \phi_0\}. \quad (10)$$

$$\mathbf{M}_{mn}^{(3)} = (m/2i) |\mathbf{M}| J_n(2\pi m \alpha / L_x) \sin \phi_0;$$

$$m = \pm 1, \quad n = 0, \pm 1, \pm 2, \dots, \quad (4c)$$

where

$$J_n(x) = \frac{1}{\pi} \int_0^\pi \exp[-i(n\theta - x \sin \theta)] d\theta, \quad (5a)$$

is the type one Bessel function of order  $n$ . The following relations will be useful in this analysis:

$$J_n(-x) = J_{-n}(x) = (-1)^n J_n(x), \quad (5b)$$

$$J_n(0) = \begin{cases} 1 & n = 0 \\ 0 & n \neq 0 \end{cases}, \quad (5c)$$

$$\sum_{n=-\infty}^{\infty} J_n^2(x) = 1. \quad (5d)$$

One can verify, with the aid of Eq. (5d), that

$$\sum_n \sum_m (|\mathbf{M}_{mn}^{(1)}|^2 + |\mathbf{M}_{mn}^{(2)}|^2 + |\mathbf{M}_{mn}^{(3)}|^2) = |\mathbf{M}|^2. \quad (6)$$

We now investigate the demagnetizing energy for the three walls in Eq. (3).

(i) In the case of the in-plane, head-to-head wall, Eqs. (1), (3a), (4), and (5b) yield

Consequently, shifting  $\phi_0$  towards  $90^\circ$  increases the perpendicular component's demagnetizing energy only by a small amount. At the same time the move towards  $\phi_0 = 90^\circ$  substantially reduces the energy of the in-plane components [second summation in Eq. (7)] because for  $n \neq 0$  all terms in the summation are proportional to  $\cos^2 \phi_0$  (again assuming  $L_y \ll L_x$ ). On balance, therefore, the move towards the perpendicular seems to facilitate the formation of zigzag boundaries in head-to-head walls. A possible remedy is the fabrication of films with in-plane anisotropy so that the gain in demagnetization is offset by anisotropy losses.

(ii) In the case of a in-plane, side-by-side wall; Eqs. (1), 3(b), (4), and (5b) yield

The optimum value of  $\phi_0$  now depends on  $h/L_x$ . The critical value is  $h/L_x = 0.255$  where  $G(h/L_x) = \frac{1}{2}$ . Below the critical point  $\phi_0 = 90^\circ$  so that the magnetization is everywhere in plane (Neel wall). Above the critical point  $\phi_0 = 0$  and the rotation of magnetization takes place outside the plane of the

film (Bloch wall). More accurate descriptions of the side-by-side walls including the effects of exchange and anisotropy can be found in Ref. 2. The introduction of the zigzag structure does not seem to reduce the energy density in Eq. (9). Thus, side-by-side walls appear to be in their state of

minimum demagnetizing energy when they are free from jaggedness.

(iii) In the case of a perpendicular wall, Eqs. (1), (3c), (4), and (5b) yield

$$E_M = \pi |\mathbf{M}|^2 \left[ \sum_{n=-\infty}^{\infty} G \left[ h \sqrt{(1/L_x)^2 + (n/L_y)^2} \right] J_n^2 \left( \frac{2\pi\alpha}{L_x} \right) + \sum_{n=-\infty}^{\infty} \left\{ 1 - G \left[ h \sqrt{(1/L_x)^2 + (n/L_y)^2} \right] \right\} J_n^2 \left( \frac{2\pi\alpha}{L_x} \right) \left( \frac{(1/L_x)^2 \cos^2 \phi_0 + (n/L_y)^2 \sin^2 \phi_0}{(1/L_x)^2 + (n/L_y)^2} \right) \right]. \quad (11)$$

In the absence of jaggedness ( $\alpha = 0$ ) we have

$$E_M = \pi |\mathbf{M}|^2 \{ G(h/L_x) + [1 - G(h/L_x)] \cos^2 \phi_0 \}. \quad (12)$$

The best choice for  $\phi_0$  is  $\phi_0 = 90^\circ$  so that the in-plane component of magnetization becomes parallel to the  $y$  axis. As  $\alpha$  increases, however,  $\phi_0$  moves towards 0, i.e., the in-plane component moves away from  $y$  towards the  $x$  axis. As can be seen from Eq. (11) the energy of the perpendicular component goes down with increasing  $\alpha$ . The contribution of the in-plane component along  $x$  is only in the  $n = 0$  term of the second sum, since (with  $L_y \ll L_x$ ) all the other terms are dominated by the component along  $y$ . By reducing  $\phi_0$ , then, we reduce the contribution of the in-plane magnetization in the  $y$  direction, while making a small sacrifice in terms of the energy of the  $x$  component.

## II. DEMAGNETIZING ENERGY IN RANDOM MAGNETIZATION DISTRIBUTIONS

Consider a random magnetization distribution  $\mathbf{M}(x, y)$  in a film of thickness  $h$  and dimensions  $L_x \times L_y$  in the limit when both  $L_x$  and  $L_y$  tend to infinity. Let us define the autocorrelation functions for the various components of magnetization as follows:

$$R_{xx}(\eta, \zeta) = \langle M_x(x_0, y_0) M_x(x_0 + \eta, y_0 + \zeta) \rangle, \quad (13a)$$

$$R_{yy}(\eta, \zeta) = \langle M_y(x_0, y_0) M_y(x_0 + \eta, y_0 + \zeta) \rangle, \quad (13b)$$

$$R_{xy}(\eta, \zeta) = \langle M_x(x_0, y_0) M_y(x_0 + \eta, y_0 + \zeta) + M_y(x_0, y_0) M_x(x_0 + \eta, y_0 + \zeta) \rangle, \quad (13c)$$

$$R_{zz}(\eta, \zeta) = \langle M_z(x_0, y_0) M_z(x_0 + \eta, y_0 + \zeta) \rangle. \quad (13d)$$

The symbol  $\langle \dots \rangle$  means statistical average over an ensemble of identical systems (films) where each member of the ensemble exhibits a particular instance of a random distribution. Stationarity is assumed by indicating the dependence of the autocorrelation functions on the relative and not the absolute positions. Stationarity gives symmetry with respect to the origin of the  $\eta\zeta$  plane to the autocorrelation functions, but other types of symmetry may also occur under special conditions.

We now calculate the statistical averages of the various terms in Eq. (1a). As expected, these averages are related to the Fourier transforms of the preceding autocorrelation

functions. For the  $z$  component of magnetization we obtain

$$\langle |\mathbf{M}_{mn} \cdot \hat{z}|^2 \rangle \approx \frac{1}{L_x L_y} \int_{-L_x}^{L_x} \int_{-L_y}^{L_y} R_{zz}(\eta, \zeta) \times \exp \left[ -i2\pi \left( \frac{m}{L_x} \eta + \frac{m}{L_y} \zeta \right) \right] d\eta d\zeta, \quad (14)$$

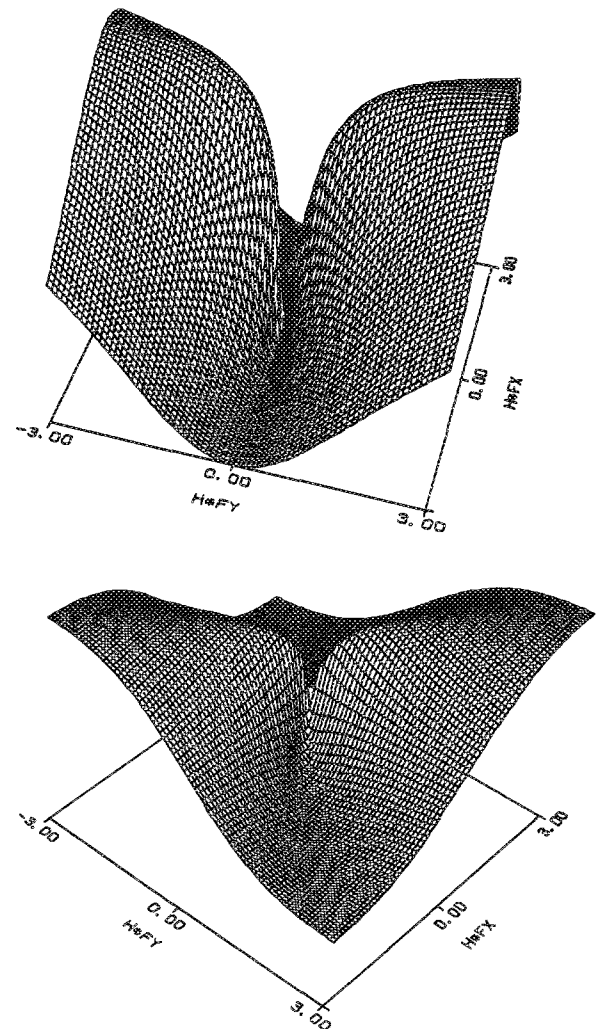


FIG. 3. Plots of  $G_{yy}(f_x, f_y)$  and  $G_{xx}(f_x, f_y)$  in the frequency plane.  $G_{xx}$  is the same as  $G_{yy}$  but rotated around the vertical axis by  $90^\circ$ .

where the approximate equality becomes exact in the limit when  $L_x$  and  $L_y$  tend to infinity. Defining the Fourier transform of  $R_{zz}(\eta, \zeta)$  as

$$\hat{R}_{zz}(f_x, f_y) = \int \int_{-\infty}^{\infty} R_{zz}(\eta, \zeta) \times \exp[-i2\pi(f_x\eta + f_y\zeta)] d\eta d\zeta, \quad (15)$$

and realizing that  $1/L_x = df_x$  and  $1/L_y = df_y$  we can write Eq. (14) as follows:

$$\langle |\mathbf{M}_{mn} \cdot \hat{\mathbf{z}}|^2 \rangle = \hat{R}_{zz}(f_x, f_y) df_x df_y. \quad (16)$$

Similarly,

$$\langle |\mathbf{M}_{mn} \cdot \hat{\sigma}|^2 \rangle = \left( \frac{f_x^2}{f^2} \hat{R}_{xx}(f_x, f_y) + \frac{f_x f_y}{f^2} \hat{R}_{xy}(f_x, f_y) + \frac{f_y^2}{f^2} \hat{R}_{yy}(f_x, f_y) \right) df_x df_y. \quad (17)$$

Consequently, in this limit of large  $L_x$  and  $L_y$ , one can write the average demagnetizing energy density as

$$\langle E_M \rangle = 2\pi \int \int_{-\infty}^{\infty} [G_{xx}(f_x, f_y) \hat{R}_{xx}(f_x, f_y) + G_{xy}(f_x, f_y) \hat{R}_{xy}(f_x, f_y) + G_{yy}(f_x, f_y) \hat{R}_{yy}(f_x, f_y) + G_{zz}(f_x, f_y) \hat{R}_{zz}(f_x, f_y)] df_x df_y, \quad (18a)$$

where

$$G_{xx}(f_x, f_y) = [f_x^2 / (f_x^2 + f_y^2)] [1 - G(hf)], \quad (18b)$$

$$G_{xy}(f_x, f_y) = [f_x f_y / (f_x^2 + f_y^2)] [1 - G(hf)], \quad (18c)$$

$$G_{yy}(f_x, f_y) = [f_y^2 / (f_x^2 + f_y^2)] [1 - G(hf)], \quad (18d)$$

$$G_{zz}(f_x, f_y) = G(hf). \quad (18e)$$

The functions  $G_{xx}$ ,  $G_{xy}$ , and  $G_{yy}$  are shown in Fig. 3.

#### ACKNOWLEDGMENT

This work has been supported by a grant from the IBM Corporation.

<sup>1</sup>M. Mansuripur and R. Giles, IEEE Trans. Magn. MAG-24, 2326 (1988).

<sup>2</sup>B. K. Middleton, in *Active and Passive Thin Film Devices*, edited by T. J. Coultts (Academic, New York, 1978), pp. 603-696.